

Experimental Demonstration of Optimal Unambiguous State Discrimination

Roger B. M. Clarke⁽¹⁾, Anthony Chefles⁽²⁾, Stephen M. Barnett⁽¹⁾ and Erling Riis⁽¹⁾

⁽¹⁾*Department of Physics and Applied Physics, University of Strathclyde, Glasgow G4 0NG, UK*

⁽²⁾*Department of Physical Sciences, University of Hertfordshire, Hatfield AL10 9AB, Herts, UK*

PACS: 03.67.k, 03.65.Bz, 42.50.-p

We present the first full demonstration of unambiguous state discrimination between non-orthogonal quantum states. Using a novel free space interferometer we have realised the optimum quantum measurement scheme for two non-orthogonal states of light, known as the Ivanovic-Dieks-Peres (IDP) measurement. We have for the first time gained access to all three possible outcomes of this measurement. All aspects of this generalised measurement scheme, including its superiority over a standard von Neumann measurement, have been demonstrated within 1.5% of the IDP predictions.

One of the major themes of the emerging subject of quantum information is the classical information bearing capabilities of quantum systems. In classical physics, different signal states are, at least in principle, fully distinguishable, although errors do occur due the practical difficulty of eliminating noise. By contrast, the identification of signals carried by quantum states will, in general, be imperfect. This a consequence of the nature of the quantum measurement process, which implies that only orthogonal states can be distinguished perfectly. Consider two parties, Alice and Bob. Alice sends Bob a system prepared in some quantum state chosen from a set $\{|\psi_j\rangle\}$ known to Bob. Bob cannot construct a measuring apparatus which will conclusively identify which state Alice sent with zero probability of error unless the states $|\psi_j\rangle$ are orthonormal.

If the states are non-orthogonal, then Bob is forced by physical law to weaken the specifications of his measurement. He can relax the condition of accuracy, in which case his measurement result will sometimes be incorrect. If the signal is in one of two possible states, $|\psi_{\pm}\rangle$, with respective a priori probabilities η_{\pm} , then the minimum error probability is given by the Helstrom bound [1]:

$$P_e(\text{opt}) = \frac{1}{2} \left(1 - \sqrt{1 - 4\eta_+\eta_-|\langle\psi_+|\psi_-\rangle|^2} \right). \quad (1)$$

Notice that this is zero only when the states are orthogonal. Minimum error measurements always identify the signal as being one of the possible states, which is to say that they are *conclusive*, although this identification will be *incorrect* with probability $P_e(\text{opt})$. The Helstrom measurement has recently been demonstrated in the laboratory [2], using weak optical pulses where the two states were non-orthogonal polarisation states.

The other option available to Bob is to drop the requirement of conclusiveness: that is, the condition that the measurement result will always announce one of the possible states. This kind of strategy was first described by Ivanovic [3], who showed that it allows two non-orthogonal states to be discriminated *without error*, but with a finite probability of getting a third and *inconclusive* result. The optimum strategy of this kind is that which minimises the probability of inconclusive results. Further work by Dieks [4] and Peres [5] established this minimum, which is given by the Ivanovic-Dieks-Peres (IDP) bound:

$$P_{\text{opt}} = |\langle \psi_+ | \psi_- \rangle|. \quad (2)$$

This bound applies when the two states appear with equal a priori probabilities. A more general bound for two states with arbitrary a priori probabilities was later obtained by Jaeger and Shimony [6].

Non-orthogonal photon polarisation states are also well-suited to the realisation of this kind of measurement. Indeed, unambiguous discrimination between non-orthogonal polarisations in the vicinity of the IDP limit has been carried out by Huttner *et al* [7]. In this experiment, linearly polarised, weak optical pulses (~ 0.1 photons/pulse) were transmitted through an optical fiber with polarisation-dependent loss. This loss was adjusted so that the photons which were not absorbed emerged in one of two orthogonal states, corresponding to the two non-orthogonal input states, which were then measured in a von Neumann measurement. Occasions when the polarisation-dependent loss resulted in photon absorption were interpreted as inconclusive results, and the inferred loss was in agreement with the IDP prediction. However, the inconclusive results could not be positively confirmed, since there were other reasons for non-detection. Also, the experiment was only performed using one pair of input states.

In this Letter, we report an implementation of unambiguous polarisation discrimination at the IDP limit using free-space interferometry, overcoming the limitations of the fiber-based implementation. Importantly, it allows total access to all output ports, particularly those corresponding to the three outcomes of the IDP measurement. The absorption in our interferometer is negligible implying that all input photons will result in either conclusive discrimination or inconclusive results in accordance with the IDP bound. Consequently, our experiment is the first full demonstration of the IDP measurement.

The measurement scheme was designed to discriminate between two non-orthogonal linear polarisation states of light. An optical interferometer using polarising beamsplitters and waveplates was used to physically separate appropriate polarisation components of the input light, manipulated them, and recombine them to perform the final measurement. Our experiment is based on a similar proposal by Huttner *et al* [7].

The states we chose to discriminate between were

$$|\psi_{\pm}\rangle = \cos\alpha|\leftrightarrow\rangle \pm \sin\alpha|\updownarrow\rangle, \quad (3)$$

where $0 \leq \alpha \leq 45^\circ$, and $|\leftrightarrow\rangle$ and $|\updownarrow\rangle$ correspond to horizontal and vertical polarisation. These states are depicted in figure 1.

Figure 1 also demonstrates that orthogonalisation of the two input polarisation states, $|\psi_+\rangle$ and $|\psi_-\rangle$, can be achieved by reducing the amplitude along $|\leftrightarrow\rangle$. Upon such a transformation, they can be distinguished perfectly by a von Neumann measurement. The remaining amplitude must not be involved in this measurement process, and corresponds to an inconclusive result. In the experiment of Huttner *et al* [7] it was this component was absorbed in the fiber cladding and could not be measured directly. In our experiment this amplitude is detected as light from one of the output ports of the interferometer.

The interferometer is shown in the uppermost part of Figure 2. Isolation of the horizontal and vertical components was performed with PBS2. PBS3 was made partially reflecting by varying the orientation of waveplate WP4. To orthogonalise the input states, the amplitude of the reflected light from PBS3 must have the same magnitude as that reflected from PBS2. The two beams are recombined in PBS5 and analysed in a von Neumann measurement using WP6 and PBS6. The outcome of this measurement is detected with photodiodes PD1 and PD2. The two path lengths through the interferometer are chosen such that input state $|\psi_+\rangle$ is detected by PD1 and input state $|\psi_-\rangle$ is detected by PD2. The transmission of PBS3 is the required reduction in the horizontal component of the input light common to both input states, and corresponds to the inconclusive result. This light was detected on PD3 and was defined as the loss required to orthogonalise the input states. We measured this loss as α was varied from 0 to 45 degrees. It can be seen from equation 2 that, theoretically, the fraction of the light measured on PD3 is $\cos 2\alpha$.

Although the alignment and stabilisation requirements of our interferometer are much more stringent than for a fiber arrangement, our apparatus offers several significant benefits. The greatest of these is full detection of the light in the three possible outcomes of the measurement. Indeed, it is necessary to be able to monitor all the output ports in

more complex experiments, for example the discrimination of trine and tetrad polarisation states [8]. Secondly, we are able to vary the induced loss along the horizontal component continuously and deterministically.

The light source was a mode-locked Ti:Sapphire laser operating at 780 nm with a repetition rate of 80.3 MHz. The pulse duration was 1 ps, corresponding to a pulse length of 300 μm . This ensured that there was only one pulse in the optical system at any one time and that the length of the pulse was much shorter than the path length of the interferometer. The output was focused with lens L1 through a 60 μm pinhole to produce a clean spherical wavefront. The light was then passed through lens L2 to produce a shallow focus on the centres of the 1 mm² photodiodes (Centronix, BPX65) beyond the interferometer, which were arranged to be of equal optical path lengths away. In this way almost 100% of the light input into the interferometer reached the detectors.

Neutral density filters were inserted to attenuate the light to an average of 0.2 photons per pulse (4 pW) at the interferometer input. Fine adjustment of the intensity was possible by rotating the waveplate WP1, placed before the Rochon polarising beamsplitter, PBS1. This type of beamsplitter was chosen for its high extinction ratio, measured to be greater than 1 part in 5000. A Wollaston type beamsplitter, PBS6, was used in the analyser part of the experiment for the same reason.

The input to the interferometer was obtained from the linearly polarised straight through beam of PBS1. The polarisation state of this input beam was changed using two half waveplates, WP2 and WP3. The first rotated the polarisation angle from 0 to 45 degrees above the horizontal, preparing the polarisation state $|\psi_+\rangle$. The second waveplate, WP3, was oriented such that it had the effect of flipping the polarisation state about the horizontal axis, transforming the input state $|\psi_+\rangle$ to $|\psi_-\rangle$. In this way, the input states were easily exchanged.

Due to the very low light levels, phase sensitive detection, using a chopper wheel, was required to recover the analogue signals from detectors 1-5. The photodiodes had a nominal quantum efficiency of 83% and were terminated by 10 M Ω , and were biased in parallel by a

single 9 V source. For light levels equivalent to 0.1 photons per pulse, the average current obtained is 1.1 pA, which equates to 11 μ V across the termination. Regular measurements were taken of the small offsets that arose when using this technique. Light levels equivalent to less than 0.01 photons per pulse were detectable.

To normalise out the amplitude noise of the Ti:Sapphire laser, a pick-off beam was measured on PD6 when *any* measurements of photodiodes 1-5 were taken. Again, phase-sensitive detection was performed, but using a separate lock-in amplifier. Photodiodes 1-5 were calibrated relative to each other to better than 1% by changing the distribution of light around the interferometer with waveplates.

The interferometer itself was constructed from four AR coated polarising beamsplitters PBS2-5 mounted on a machined monolithic aluminium block. The optical pathlength difference in the two arms was inferred to be less than 4 μ m over the 80 mm total pathlength from the extinction ratio obtained when used in a Mach-Zehnder operation. PBS5 was capable of being rotated around and translated along all axes with piezo-electric transducers. The AR coated $\lambda/2$ waveplates used were measured to maintain the linearity of polarisation to 1 part in 2000.

The fringe visibility of the interferometer when used in a conventional Mach-Zehnder operation was measured to be better than 200:1. The translational and angular stability of the interferometer was inferred to be less than 100 nm and 0.001 degrees respectively over at least half an hour. This level of stability was vital when taking results over the prolonged periods of time needed when using phase sensitive detection.

Calibration of the beamsplitters was performed to determine their polarisation properties. This was particularly important for understanding the results for small α . A small amount of birefringence of the beamsplitters meant that for horizontally polarised input light, the transmitted power was comprised of 98.2% horizontally and 0.9% vertically polarised light. The remaining power was reflected and almost equally distributed between the two polarisation components. Approximately the same leakages were found for vertically polarised input light.

To align the interferometer the input was set to $|\psi_+\rangle$, $\alpha = 45$ degrees, and WP4 set so that PBS3 reflected all the light (zero loss ideally). This resulted in equal amplitudes of light reaching PBS5 from each arm, corresponding to a conventional Mach-Zehnder interferometer. The path lengths and angles were varied using PBS5 to obtain the maximum visibility of the interference. When this occurred, the signal from PD2 was at a minimum.

The experiment was performed by preparing the input state $|\psi_+\rangle$ in approximately 4 degrees steps from $0 \leq \alpha \leq 45$ degrees. The exact angle was inferred by measuring the light in each arm immediately after PBS2 using all the detectors. High input powers were used to obtain a good signal to noise ratio. The light transmitted through PBS3 was then varied by rotating WP4 such that the signal from PD2 was at a minimum. The measured signal at PD2 is defined as the measured error rate since in theory 100% of the light should reach PD1. In practice, it is non-zero due to experimental imperfections.

The fraction of transmitted light through PBS3 was measured classically as the fraction of the total power incident on PD3 and the sum of the outputs of all the other photodiodes.

The transmittance of PBS3 was varied, using WP4, to obtain the minimum signal on PD2 at high light levels. It was verified that this minimum was obtained using the same angle of WP4 at any light level, including 0.2 photons per pulse. High light levels were therefore used to ensure a high signal to noise ratio in PD2 to obtain the best measure of the transmittance of PBS3.

The intensity was then reduced to 0.2 photons per pulse and the error rate, on PD2, measured. Given the extremely low light levels in PD2 (typically 0.01 photons per pulse or 0.2 pW), the measurement error of $\pm 2.5\%$ of the total light detected was comparable to the signal expected at this port. Therefore the extinction ratio of 1 in 200 could not be observed at these power levels. For $\alpha < 15^\circ$, the amplitude of the light entering the interferometer was increased up to a maximum of 1 photon per pulse in order that an error rate could be measured.

The input state was then changed from $|\psi_+\rangle$ to $|\psi_-\rangle$ by inserting WP3. The error rate, the signal measured on PD1 this time, was measured with no other alteration to the

apparatus. The alignment of the interferometer was checked after changing the angle α for the next pair of states $|\psi_+\rangle$ and $|\psi_-\rangle$.

Figure 3 shows the light on PD3, the induced loss, needed to produce the minimum error rate of distinguishment against α , for $0 < \alpha < 45$ degrees. The RMS deviation from the ideal theoretical curve is 1.3%, clearly validating the Ivanovic-Dieks-Peres measurement scheme. The error in PD3 was estimated by rotating WP4 until the signal on PD1 increased noticeably. For angles less than 30 degrees the sensitivity became so great that this error could not be estimated quantitatively and the uncertainty is less than the size of the points in the figure. A model based upon the measured characteristics of the PBS's, described in the next paragraph, reproduces the experimental results within the estimated error values.

The error rates obtained with incident angle are plotted in figure 4. The states $|\psi_+\rangle$ and $|\psi_-\rangle$ are shown at the same angle position. Also plotted is error rate associated with the best possible von Neumann measurement (Eq. 1 with $\eta_1 = \eta_2 = \frac{1}{2}$). Our data clearly shows error probabilities that are below this level. For $14^\circ < \alpha < 45^\circ$ the average experimental error rate for the two input states is 2.8%. For smaller angles the error rate rises significantly. We modelled the behaviour of the interferometer using non-ideal PBS's based on the calibration data obtained previously (no phase information was available and we assumed 0 and 90 degrees phase changes upon transmission and reflection respectively). The experimental procedure was followed, optimising the loss for state $|\psi_+\rangle$ and then flipping to state $|\psi_-\rangle$ to obtain the error rates. These results are also shown in Figure 4 and are in good qualitative agreement with the experimental results. For small α , the leakages of the PBS's are such that the errors present are of comparable size to the ideal signals.

We have clearly demonstrated the IDP measurement scheme using a free space interferometer. For the first time the loss required to obtain unambiguous state discrimination was confirmed by direct measurement and found to be consistent with the ideal theoretical values at the 1% level. The low light levels used, typically 0.2 photons per pulse, were the limiting factor in measuring the error rate for $\alpha > 14^\circ$. We have shown that for angles smaller than this the performance of the polarising beamsplitters is the limiting factor.

This work was funded by the UK Engineering and Physical Sciences Research Council.

- [1] C. W. Helstrom, *Quantum Detection and Estimation Theory*, (Academic Press, New York, 1976).
- [2] S. M. Barnett and E. Riis, *J. Mod. Opt.* **44** 1061 (1997).
- [3] I. D. Ivanovic, *Phys. Lett. A* **123** 257 (1987).
- [4] D. Dieks, *Phys. Lett. A* **126** 303 (1988).
- [5] A. Peres, *Phys. Lett. A* **128** 19 (1988).
- [6] G. Jaeger and A. Shimony, *Phys. Lett. A* **197** 83 (1995).
- [7] B. Huttner, A. Muller J. D. Gautier, H. Zbinden and N. Gisin, *Phys. Rev A* **54** 3783 (1996).
- [8] R. B. M. Clarke, V. M. Kendon, A. Chefles, S. M. Barnett, E. Riis and M. Sasaki , submitted to *Phys. Rev A*

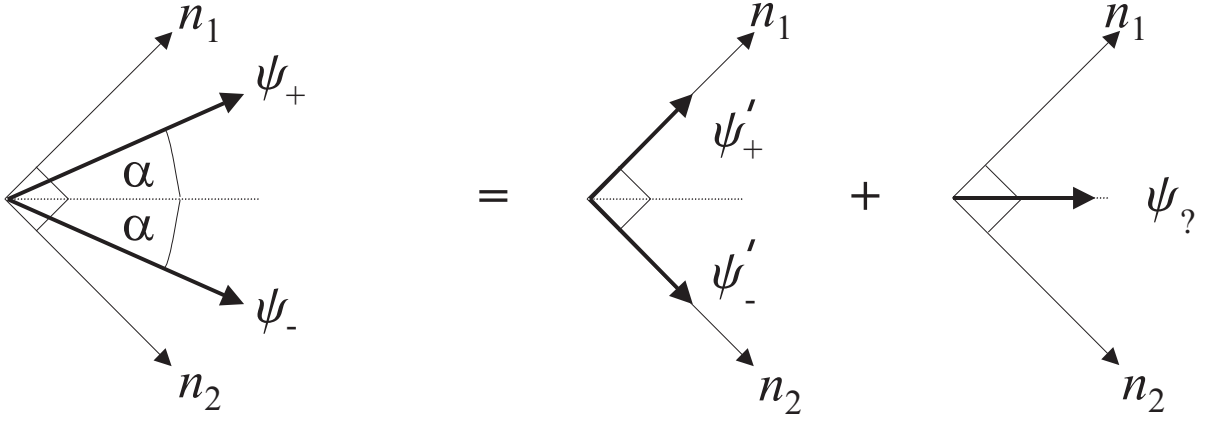


FIG. 1. The components of the states $|\psi_+\rangle$ and $|\psi_-\rangle$ can be separated to form two auxiliary states, $|\psi'_+\rangle$ and $|\psi'_-\rangle$, and a common state $|\psi_?\rangle$. $|\psi'_+\rangle$ and $|\psi'_-\rangle$ can be discriminated perfectly by a von Neumann measurement along the orthogonal basis vectors n_1 and n_2 . $|\psi_?\rangle$ is common to both initial states and corresponds to an inconclusive result.

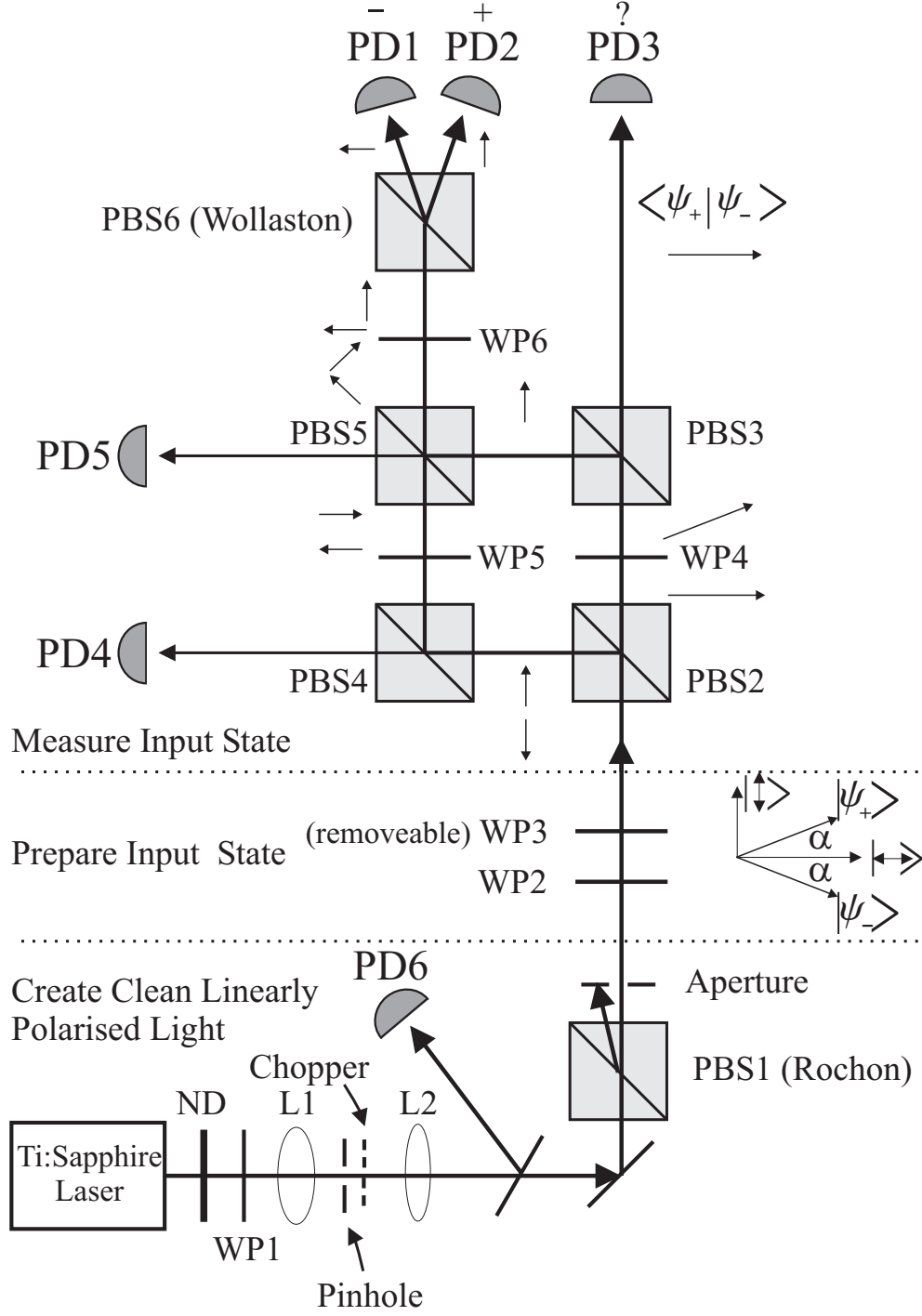


FIG. 2. Experimental setup to prepare, process and discriminate the states $|\psi_+\rangle$ and $|\psi_-\rangle$. See text for full description. L = lens, ND = neutral density filter to attenuate the light, PD = photodiode, WP = waveplate, all $\lambda/2$, to rotate the polarisation of the light. PBS = polarising beam splitter, all reflect vertical polarisation and transmit horizontal polarisation.

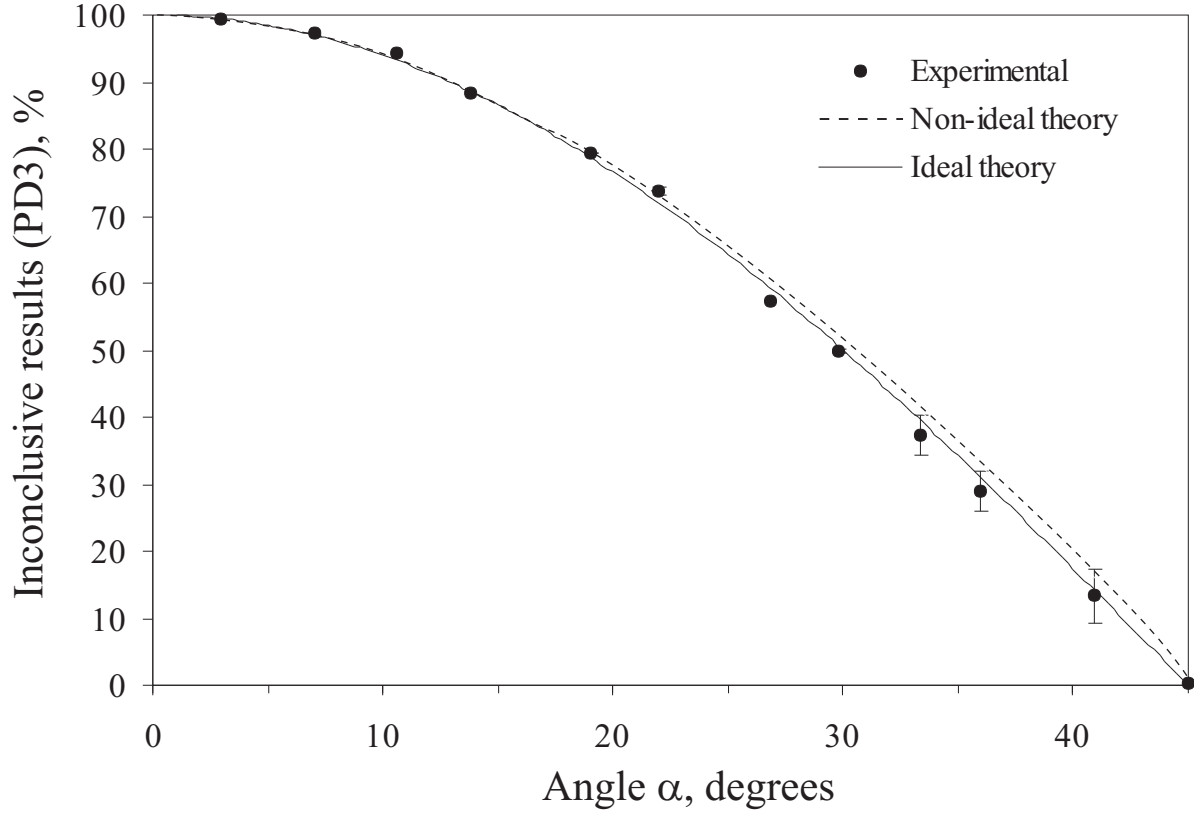


FIG. 3. The dark points show experimental signal detected on PD3, corresponding to inconclusive results, required to orthogonalise the input states. The errors are derived from the maximum possible deviation required to observe a significant increase in the discrimination error rate. The continuous curve shows the ideal theoretical values for the inconclusive loss rates, $\cos 2\alpha$. A model using the characteristics of the non-ideal beamsplitters was used to generate the dashed curve. The estimated error of this line is approximately twice the experimental error, and was derived by optimising the extinguishment of the signal on PD2 to the 0.1% level.

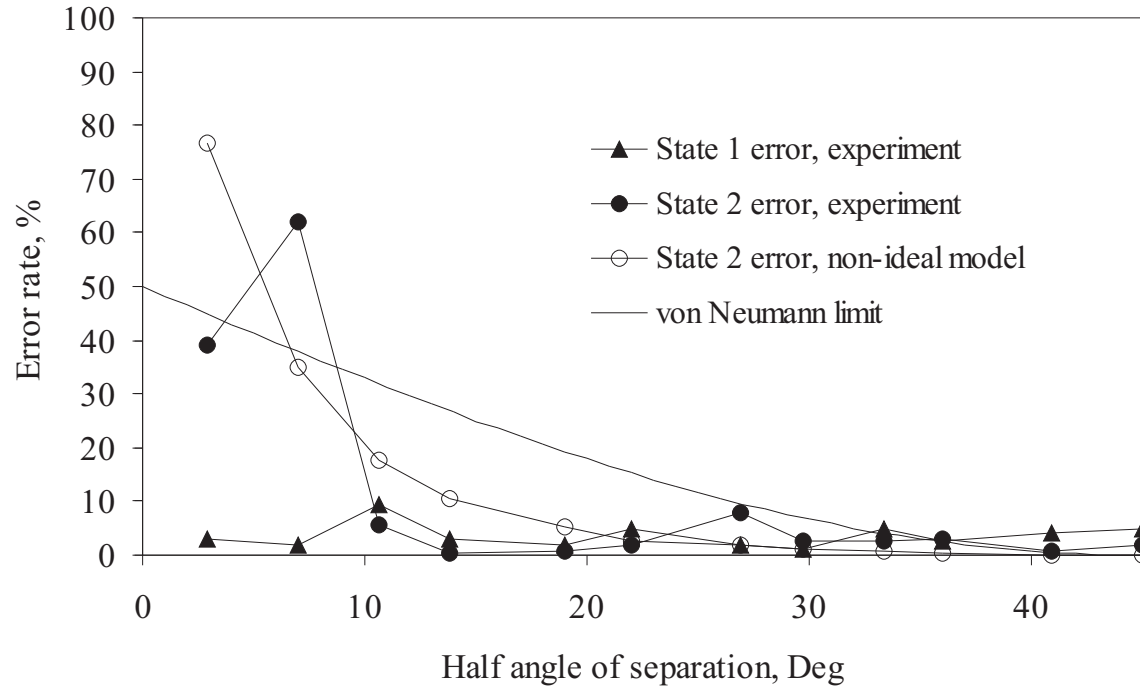


FIG. 4. The experimentally observed error rates (PD2 and PD1) obtained with input states $|\psi_+\rangle$ and $|\psi_-\rangle$ respectively. Also shown is the theoretical model using non-ideal beamsplitters with the same characteristics as in the experiment, and the best possible von Neumann error rate.